Electronic Supplementary Material (ESI) for Dalton Transactions.
This journal is © The Royal Society of Chemistry 2022

Supporting Information

Selective Hydrogenolysis of 5-Hydroxymethylfurfural to 2,5-Dimethylfuran Over Cobalt Nanoparticles Inlaid Cobalt Phyllosilicate

Lixia Sun [a], Shangyang Li [a], Zhuoyou Gao [a], Shutao Gao [a], Wei Gao [a], Xiang Cheng [a], Ningzhao Shang [a,*], Yongjun Gao [b,*], Chun Wang [a,*]

[a] College of Science, Hebei Agricultural University, Baoding 071001, China

[b] College of Chemical and Environmental Science, Hebei University, Baoding 071000, China

Catalyst Characterization

The high resolution transmission electron microscopy (HRTEM) were acquired on JEOL model JEM-2011IJHR) at 200 kV with an electron acceleration energy of 200 kV to observe the size and morphology of the nanoparticles. Fourier-transform infrared spectra (FT-IR) were recorded on a Bruker Tensor 27 spectrometer at room temperature. The samples were finely ground and dispersed in KBr to make pellets for FT-IR characterizations. All spectra were recorded in the range of 4000-400 cm^{-1} with a resolution of 4 cm^{-1}. The X-ray diffraction (XRD) patterns of the catalyst were collected at a Rigaku D/max 2500 X-ray diffractometer using Cu Kα radiation (40 kV, 150 mA). X-ray photoelectron spectroscopy spectra were performed on an ESCA Lab 250 (Thermo) spectrometer (Shanghai, China) using a monochromatic Al Kα (1486.6 eV) as an excitation source. The surface area, total pore volume and pore size distribution of the catalyst were measured at −196 ^{o}C using N_2 adsorption with V-Sorb 2800P volumetric adsorption equipment (Jinaipu, China). The specific surface area was calculated using the Brunauer-Emmett-Teller (BET) method, and the pore size distributions were measured using Barrett-Joyner-Halenda (BJH) analysis from the desorption branch of the isotherms. Product analysis was carried out on a Shimazdu 2014C series gas chromatograph (GC) equipped with a flame ionization detector (FID). All the separations were performed on a HP-5 capillary column (30 m × 0.32 mm i.d. × 0.25 μm film thickness). The metal content of the materials was analyzed by a T.J.A. ICP-9000 type inductively coupled plasma atomic emission spectroscopy (ICP-AES) instrument.

Temperature-programmed reduction of hydrogen (H_2-TPR) test was carried out on the Micromeritics Autochem II 2920 instrument. The sample (50 mg) was pretreated at 200 ^{o}C for 30 min h Ar flow (30 mL/min) to remove the adsorbed water and impurities. After cooling to 40 ^{o}C, the catalyst was heated to 750 ^{o}C at a rate of 10 ^{o}C/min under a 10% H_2-Ar (50 mL/min) gas mixture; the TCD signal continuously recorded.

Temperature-programmed reduction of NH_3 (NH_3-TPD) test was also carried out on the Micromeritics Autochem II 2920 instrument. The catalysts (100 mg) were reduced in H_2 at 500 °C for 2 h, after cooled to room temperature, saturated with NH_3 for 30 min, and then purged with Ar to remove the physisorbed NH_3 at 100 °C for 30 min. Subsequently, the catalysts were heated to 700 °C with a rate of 10 ^{o}C/min.

Pyridine adsorbed IR (Py-IR) spectra of powder samples were recorded with a Vertex 70 (Bruker)

FTIR spectrophotometer in the range of 4000-400 cm^{-1} at a resolution of 4 cm^{-1}. The samples were degassed in a vacuum condition at 300 °C for 1 h for the calcined sample and reduced at 500 °C for 2 h for the reduced catalyst. The samples were then exposed to pyridine after cooling down to 30 °C. The spectra were recorded at 200 °C after pretreated in vacuum for 30 min.

The thermal stability of the material was measured from room temperature to 750 °C on a thermogravimetric analyzer (TGA) (Henven HCT-2, Beijing, China).

Conversion and selectivity calculation for HDO of HMF

Conversion was calculated by the equation 1:

(1):

$$Conversion = \left(1 - \frac{mole\ of\ substrate\ after\ reaction}{mole\ of\ substrate\ before\ reaction}\right) \times 100\%$$

Selectivity was calculated by the equation 2:

(2):

$$Selectivity = \frac{mole\ of\ desired\ product}{mole\ of\ substrate\ before\ reaction - mole\ of\ substrate\ after\ reaction} \times 100\%$$

Turn over number (TON) and Turn over frequency (TOF) were calculated and defined as follows:

$$TON = \frac{Moles\ of\ substrate\ consumed}{Molar\ amount\ of\ metal\ Co} \times 100\%$$

$$TOF = \frac{Moles\ of\ substrate\ consumed}{Molar\ amount\ of\ metal\ Co\ *\ Reaction\ time} \times 100\%$$

The initial TOF was calculated at 20 min of the reaction.

Table S1. Surface area and pore size of the catalysts

Catalyst	Surface area [a] (m^2/g)	Pore size (nm)		Pore volume (cm^3/g)	
		SF [b]	BJH [c]	SF [d]	BJH [e]
CoSi-PS	232	0.89	11.44	0.079	0.60
10%CoSi-PS	226	0.84	11.35	0.078	0.62
CoSi-IMP	214	0.77	4.22	0.073	0.93
Co/Al_2O_3	124	0.79	6.05	0.043	0.22
Co/SiO_2	218	0.85	12.6	0.090	1.20

[a] BET surface area. [b] SF Median pore width. [c] BJH Adsorptiom average pore width (4V/A). [d] SF micropore volume. [e] BJH Adsorption cumulative volume

Table S2. Surface area and pore size of the catalysts

Catalyst	Surface area [a] (m^2/g)	Pore size (nm)		Pore volume (cm^3/g)	
		SF [b]	BJH [c]	SF [d]	BJH [e]
CoSi-PS-P	262	0.73	11.00	0.080	0.62
CoSi-PS-C	253	0.76	10.70	0.075	0.58
CoSi-PS	232	0.89	11.44	0.079	0.60

Analysis of HMF by GC-FID

Product analysis was carried out on a Shimazdu 2014C series gas chromatograph (GC) equipped with a flame ionization detector (FID). All the separations were performed on a HP-5 capillary column (30 m × 0.32 mm i.d. × 0.25 μm film thickness).

Conditions: 1 min hold at 60 °C, heating rate 20 °C/min from 60 °C to 270 °C, 3 min hold at 270 °C; Injector: 250 °C; Detector: FID, 280 °C.

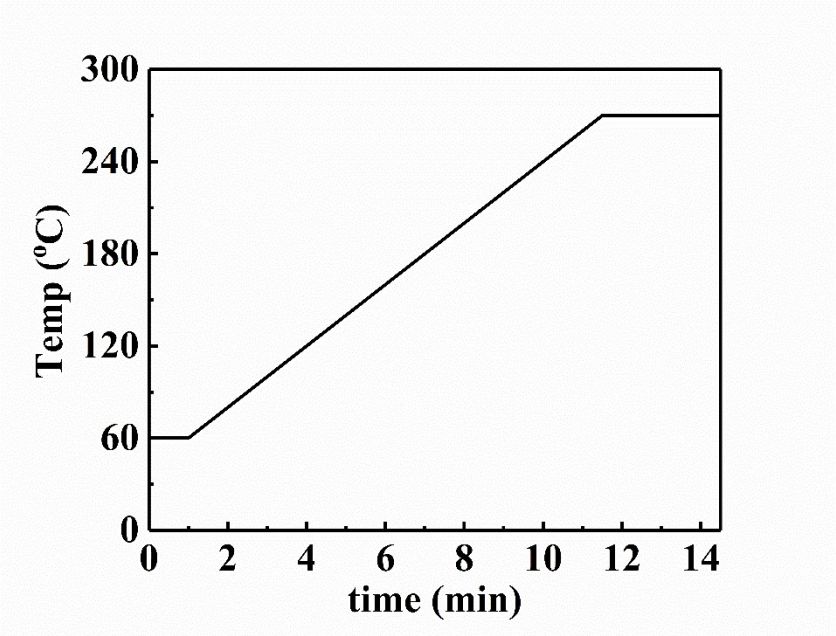

Temperature profile for GC analysis.

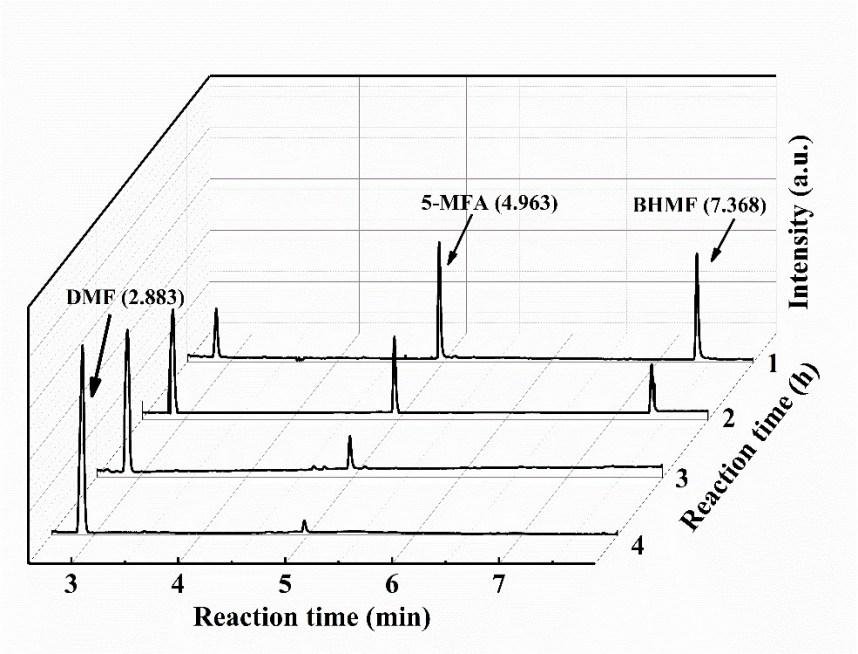

GC-FID chromatograms of the liquid products obtained from the HDO of HMF over CoSi-PS at different times

Table S3. Catalytic performance of the reported catalysts for the HDO of HMF to DMF.

Entry	Catalyst	T/°C	Pressure /MPa	H source	Time /h	Solvent	Yield/%	Reported year	Ref.
1	NiAl-850	180	1.2	H_2	4	1,4-dioxane	91.5	2015	1
2	Ni_2-Fe_1/CNTs	200	3	H_2	3	n-butanol	91.3	2015	2
3	CuZn-2	220	1.5	H_2	5	1,4-dioxane	91.8	2015	3
4	NiSi-PS	150	1.5	H_2	3	THF	DMF (64.1) + DMTHF (26.1)	2015	4
5	Ni-OMD3	200	3	H_2	6	H_2O	97.7	2016	5
6	$CuCo^R$/NGr/α-Al_2O_3	180	2	H_2	16	THF	>98	2016	6
7	Cu-Co@C	180	5	H_2	8	ethanol	99.4	2017	7
8	RuCo/CoOx	200	0.5	H_2	2	1,4-dioxane	98.5	2018	8
9	Pd/C	170	2	H_2	4	isopropanol	98	2018	9
10	Co@Cu/3CoAlOx	180	1	H_2	5	1,4-dioxane	98.5	2019	10
11	Co_3O_4	170	1	H_2	12	1,4-dioxane	83.3	2019	11
12	5% Cu−15% Ni/BC	220	4	H_2	12	THF	98.5	2019	12
13	$Fe_{0.8}Co_{3.0}Ni_{1.9}$/h-BN	180	2	H_2	4.5	THF	94	2020	13
14	5Ni-7MoS_2/mAl_2O_3	130	1	H_2	6	isopropanol	95	2020	14
15	Co@N1Gs-700	200	2	H_2	6	ethanol	94.6	2020	15
16	Cu/Al_2O_3	150	2	H_2	10	THF	93.9	2020	16
17	Co-N-C/NiAl-MMO	170	1.5	H_2	6	THF	99.9	2020	17
18	Cu/ZnO-Al_2O_3	180	1.2	H_2	5	THF	90.1	2021	18
19	Co/Mix-ZrO_2	130	1	H_2	2	THF	90.7	2021	19
20	CoSi-PS	170	1.5	H_2	4	THF	97.5	This work	

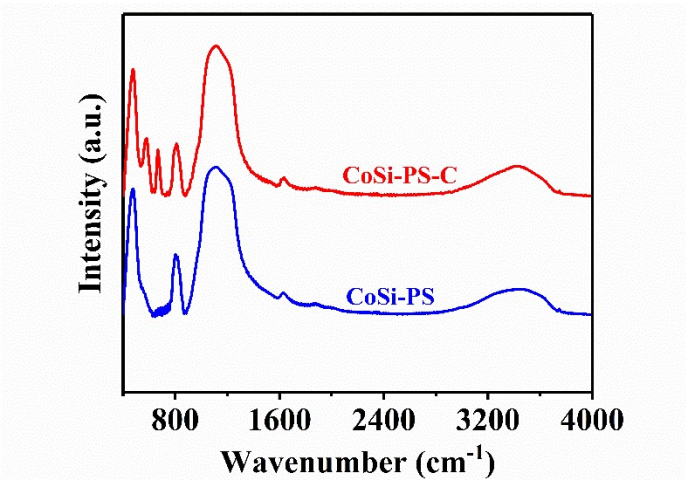

Figure S1. FT-IR results of calcined and reduced CoSi-PS catalysts

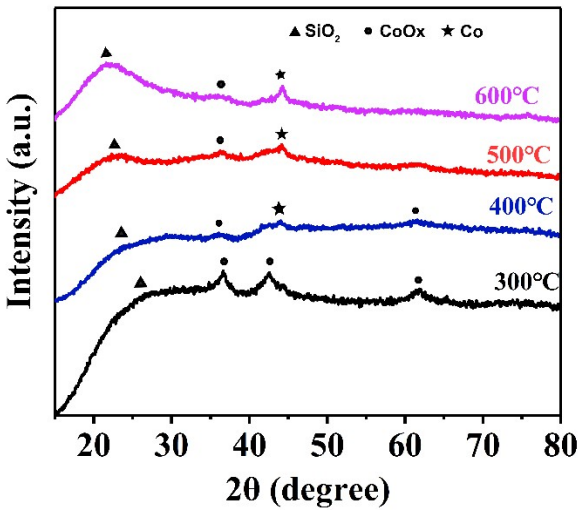

Figure S2. XRD patterns of CoSi-PS at different temperatures.

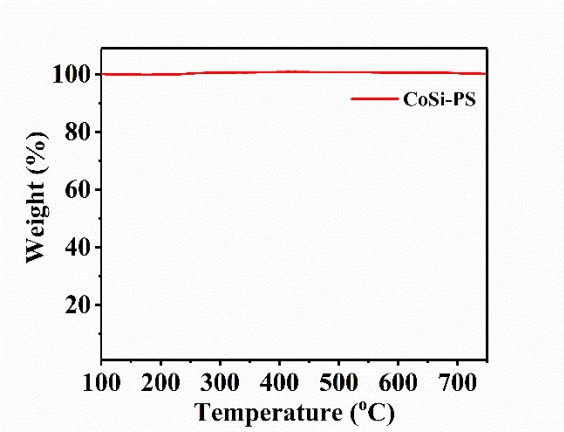

Figure S3. TGA profiles of CoSi-PS catalysts

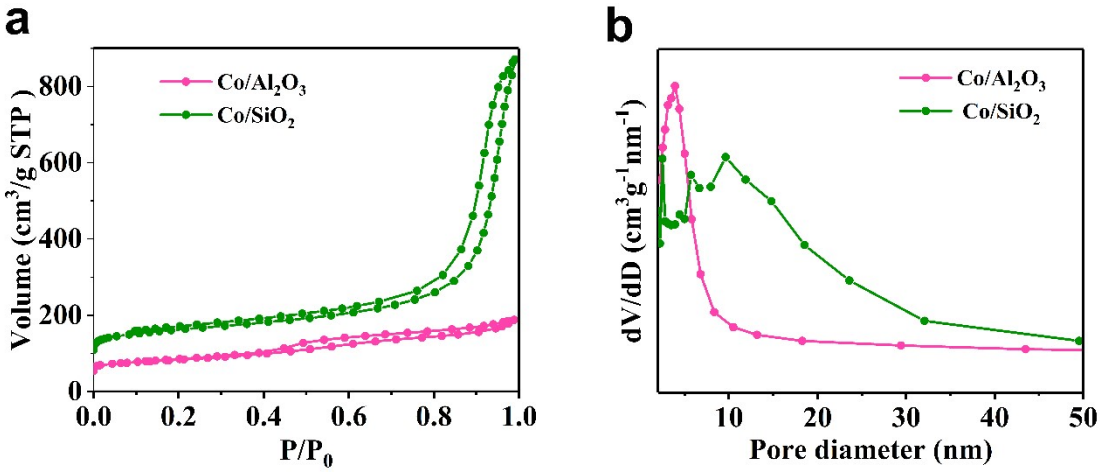

Figure S4. (a) N_2 adsorption-desorption isotherms and (b) pore size distribution of the catalysts.

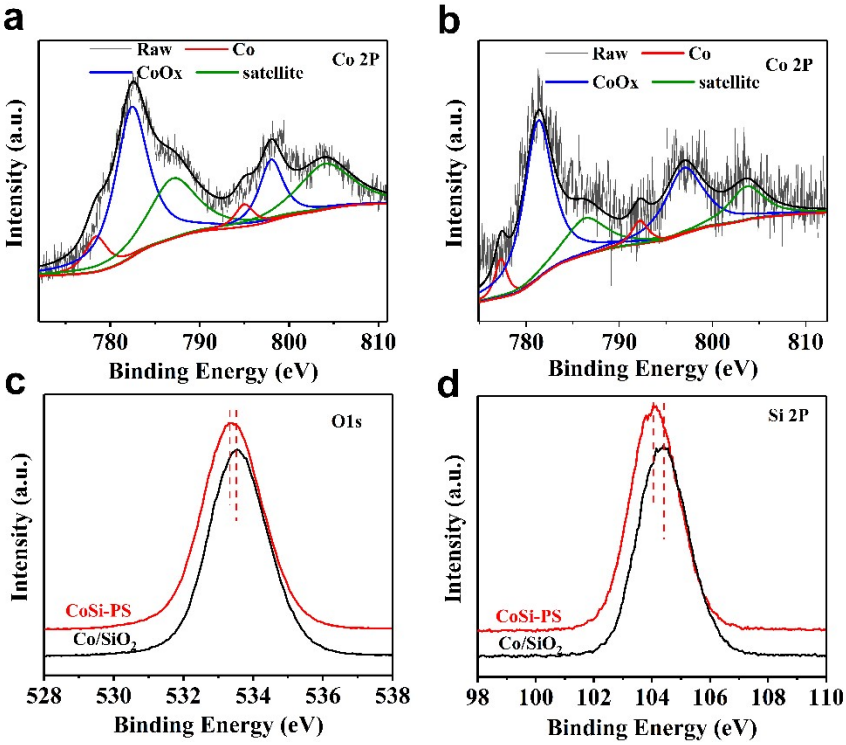

Figure S5. Co 2p spectra of CoSi-PS (a) and Co/SiO_2 (b) catalysts; O1s spectra (c) and Si 2p (d) spectra of CoSi-PS and Co/SiO_2 catalysts.

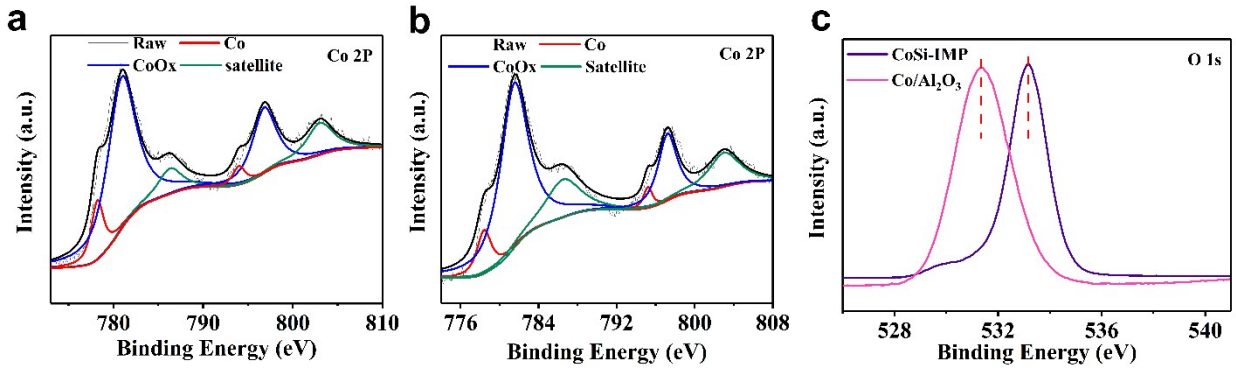

Figure S6. Co 2p spectra of CoSi-IMP (a) and Co/Al_2O_3 (b) catalyst; O1s spectra (c) of CoSi-IMP and Co/Al_2O_3 catalysts.

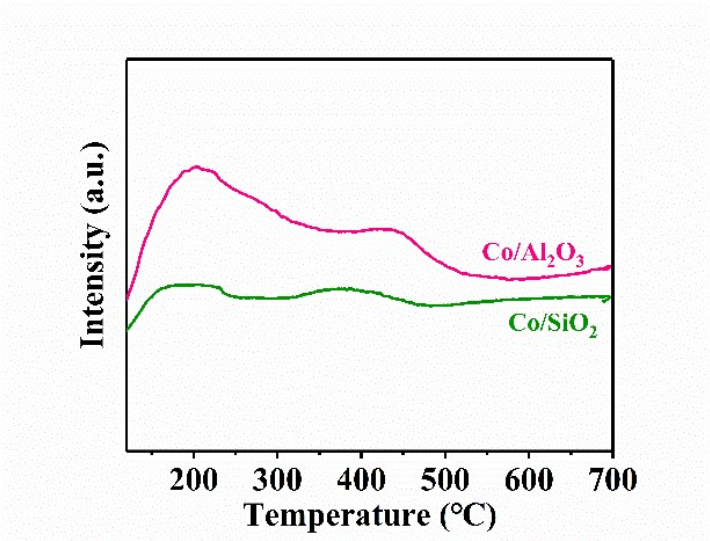

Figure S7. NH_3-TPD profiles of Co/Al_2O_3 and Co/SiO_2 catalysts

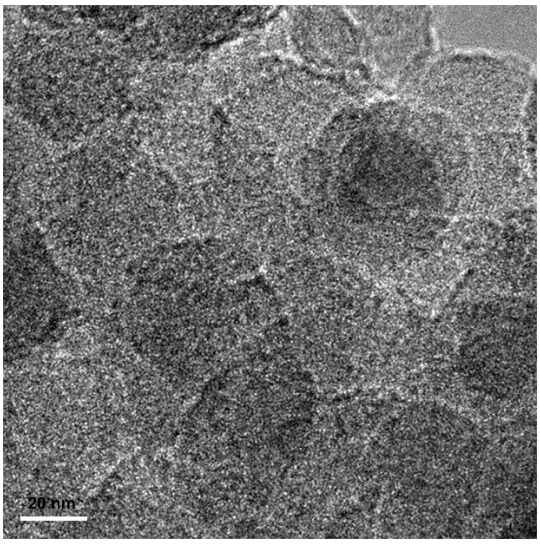

Figure S8. HRTEM images of the used CoSi-PS.

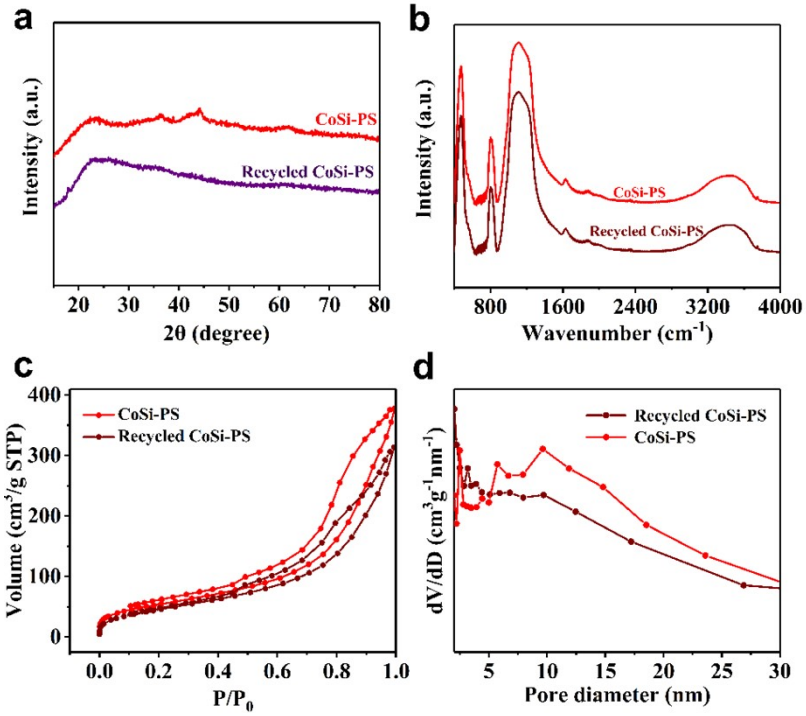

Figure S9. XRD (a), FT-IR (b), N_2 adsorption-desorption isotherm (c) and distribution of pore diameter (d) for CoSi-PS and the recycled CoSi-PS.

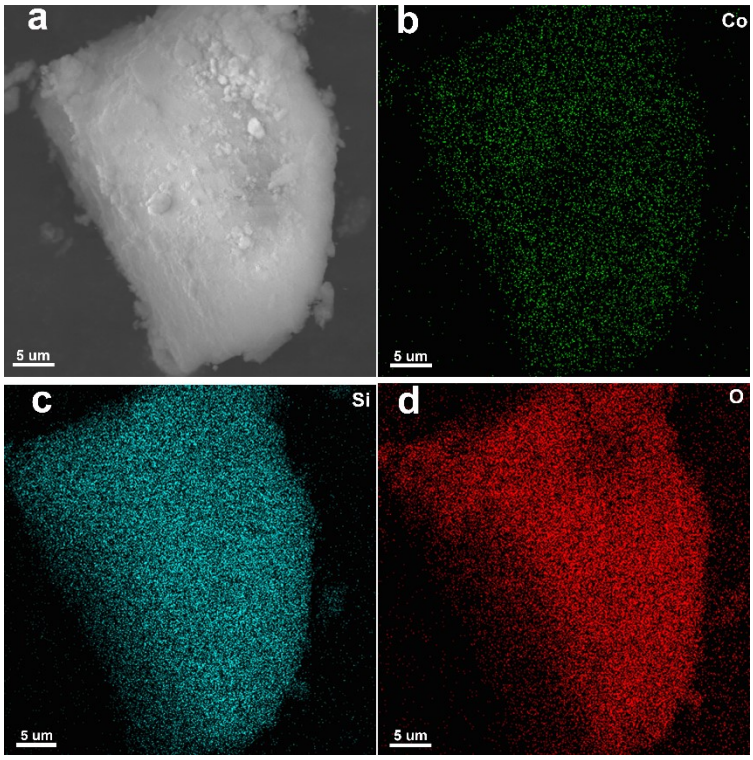

Figure S10. ADF-SEM elemental mapping of (a) the corresponding SEM of the recycled CoSi-PS catalyst, (b) cobalt, (c) silicon, (d) oxygen.

References:

1. X. Kong, R. Zheng, Y. Zhu, G. Ding, Y. Zhu and Y.-W. Li, *Green Chem.*, 2015, **17**, 2504-2014.
2. L. Yu, L. He, J. Chen, J. Zheng, L. Ye, H. Lin and Y. Yuan, *ChemCatChem*, 2015, **7**, 1701-1707.
3. Y. Zhu, X. Kong, H. Zheng, G. Ding, Y. Zhu and Y.-W. Li, *Catal. Sci. Technol.*, 2015, **5**, 4208-4217.
4. X. Kong, Y. Zhu, H. Zheng, X. Li, Y. Zhu and Y.-W. Li, *ACS Catal.*, 2015, **5**, 5914-5920.
5. R. Goyal, B. Sarkar, A. Bag, N. Siddiqui, D. Dumbre, N. Lucas, S. K. Bhargava and A. Bordoloi, *J. Catal.*, 2016, **340**, 248-260.
6. W. Guo, H. Liu, S. Zhang, H. Han, H. Liu, T. Jiang, B. Han and T. Wu, *Green Chem.*, 2016, **18**, 6222-6228.
7. B. Chen, F. Li, Z. Huang and G. Yuan, *Appl. Catal. B: Environ.*, 2017, **200**, 192-199.
8. G. Zhi, F. Guoli, L. Mengran, Y. Lan and L. Feng, *Appl. Catal. B: Environ.*, 2018, **237**, 649-659.
9. B. S. Solanki and C. V. Rode, *Journal of Saudi Chemical Society*, 2018, **23**, 439-451.
10. Q. Wang, J. Feng, L. Zheng, B. Wang and D. Li, *ACS Catal.*, 2019, **10**, 1353-1365.
11. D. Li, Q. Liu, C. Zhu, H. Wang, C. Cui, C. Wang and L. Ma, *Journal of Energy Chemistry*, 2019, **30**, 34-41.
12. C. Zhu, H. Wang, H. Li, B. Cai, W. Lv, C. Cai, C. Wang, L. Yan, Q. Liu and L. Ma, *ACS Sustain. Chem. Eng.*, 2019, **7**, 19556-19569.
13. N. Chen, Z. Zhu, T. Su, W. Liao, C. Deng, W. Ren, Y. Zhao and H. Lü, *Chem. Eng. J.*, 2020, **381**, 122755.
14. W. Han, M. Tang, J. Li, X. Li, J. Wang, L. Zhou, Y. Yang, Y. Wang and H. Ge, *Appl. Catal. B: Environ.*, 2020, **268**, 118748.
15. J. Wang, Q. Wei, Q. Ma, Z. Guo, F. Qin, Z. R. Ismagilov and W. Shen, *Appl. Catal. B: Environ.*, 2020, **263**, 118339.
16. L. M. Esteves, M. H. Brijaldo, E. G. Oliveira, J. J. Martinez, H. Rojas, A. Caytuero and F. B. Passos, *Fuel*, 2020, **270**, 117524.
17. N. Ma, Y. Song, F. Han, G. I. N. Waterhouse, Y. Li and S. Ai, *Catal. Sci. Technol.*, 2020, **10**, 4010-4018.
18. Q. Wang, Z. Yu, C. Feng, P. Fornasiero, Y. He and D. Li, *ACS Sustain. Chem. Eng.*, 2020, **8**, 15288-15298.
19. T. Xiao, X. Liu, G. Xu and Y. Zhang, *Appl. Catal. B: Environ.*, 2021, **295**, 120270.